Magazine of Civil Engineering

ISSN 2712-8172

journal homepage: http://engstroy.spbstu.ru/

Research article

UDC 691.3

DOI: 10.34910/MCE.124.5

Cementless binder based on high-calcium fly ash with calcium nitrate additive

K. Usanova[1] ✉, ***Yu.G. Barabanshchikov***[1], ***S. Dixit***[2, 3, 4]

[1] *Peter the Great St. Petersburg Polytechnic University, St. Petersburg, Russian Federation*
[2] *Division of Research, Uttaranchal University, Dehradun, India*
[3] *Division of Research and Development, Lovely Professional University, Phagwara, Punjab, India*
[4] *Khalifa University, Abu Dhabi, United Arab Emirates*

✉ *plml@mail.ru*

Keywords: fly ash, microsilica, silica fume, early strength agent, calcium nitrate, X-ray diffraction analysis, strength, heat release, differential thermal analysis, heat of hydration, phase composition

Abstract. Fly ash from Berezovskaya Thermal Power Plant, containing a lot of CaO, in combination with silica fume does not expand and exhibits the properties of a binder. However, the strength of this binder is low. The addition of $Ca(NO_3)_2$ significantly increases the strength of the binder. The work aims to study the effect of $Ca(NO_3)_2$ additive on the strength, heat of hydration, and phase composition of hydration products of the binder based on high-calcium fly ash and silica fume. The results of X-ray diffraction and Differential Thermal Analysis show that the main phases formed during the hydration of binder with the calcium nitrate additive in various dosages are lime, calcium hydroxide, ettringite, CSH(II) type silicates and calcium aluminosilicates, corresponding to such minerals as gismondine, yugavaralite, goosecreekite. When hardening in water, the residual amount of lime after 7 days is sharply reduced. An increase in the dosage of $Ca(NO_3)_2$ from 1.5 to 11.8 % leads to a decrease in the CaO content by almost 2 times. With an increase in the dosage of calcium nitrate, the content of portlandite noticeably decreases, and a significant increase in the amount of calcium hydroaluminosilicates, especially the composition of CAS_2H_4, is observed. A study of the heat release process showed that calcium nitrate greatly accelerates the process in the first 60 minutes of hydration. However, then the composition with the addition of $Ca(NO_3)_2$ is inferior in the rate of heat release to binder without the additive. When testing a mortar with polyfractional sand, the addition of $Ca(NO_3)_2$ more than doubled the compressive strength of the mortar.

Funding: Russian Science Foundation No. 21-19-00324, https://rscf.ru/project/21-19-00324/

Citation: Usanova, K., Barabanshchikov, Yu.G., Dixit, S. Cementless binder based on high-calcium fly ash with calcium nitrate additive. Magazine of Civil Engineering. 2023. 124(8). Article no. 12405. DOI: 10.34910/MCE.124.5

1. Introduction

Numerous theoretical and practical studies, as well as world experience, show that industrial waste is a suitable raw material for replacing natural resources in the construction industry [1–7]. Such wastes include wastes from coal combustion at thermal power plants, blast-furnace slags and fly ash [8, 9]. A well-known solution to obtain cementless binders is also the use of fly ash [10–12].

Due to the limited supply of class “F” fly ash in the building materials market, there is a growing interest in high calcium fly ash [13, 14]. Recently, much research has been done on the use of high-calcium fly ash to produce cementless binders. Studies show that fly ash with a high content of calcium oxide has a low degree of polymerization of silicate anions and a high content of free lime, so it has a high hydration

activity and a large volume expansion upon hydration. Because the free lime crystal size in the high calcium oxide fly ash is smaller and the lattice distortion is greater, the development of expansion during hydration of this fly ash is faster. It can be made into an effective additional binder with some appropriate technical measures [15].

It has been established that three types of fly ash from the Kansk-Achinsk fuel and energy complex provide the possibility of obtaining cementless compositions with a strength of up to 35–36 MPa. It has been shown that the additional introduction of silica fume and salt effluents into the ash stone modifies the phase composition of neoformations and the microstructure, transforming it into a denser one due to the formation of new compounds in the system – gyrolite and hydrochloraluminates [16]. The features of formation of the composition and hydraulic activity of high-calcium fly ash obtained by burning Kansk-Achinsk brown coals are studied. Fly ash, selected in a dry state, can be used as a kind of binding agents, provided that they are pre-treated, which reduces the uneven change in the volume of the fly ash paste during hydration [17].

Expansion studies of a mixture of cement and mineral admixtures show that "F" class fly ash increases the expansion of cement pastes, while "C" class fly ash and silica fume decrease expansion [18]. Studies of the fly ash hydration products from the circulating fluidized bed show that the expansion of the hardened paste occurs mainly due to the formation of dihydrate gypsum and ettringite. In addition, free lime indirectly causes expansion due to its effect on ettringite crystallization [19]. There are three hypotheses that explain the mechanism of action of fly ash to enhance the expansion of mixtures. The first hypothesis is that expanding mixtures containing fly ash produce more ettringite than mixtures without fly ash. The second hypothesis is that the lower stiffness of concrete containing fly ash results in higher expansion. The third hypothesis says that fly ash delays the hydration of expanding compounds in mixtures [20].

The reactions of hydration of expanding type K cement pastes and the effect of silica fume have been studied. In pastes with and without silica fume, expansion is associated with the formation of ettringite. The expansion continues until ettringite is formed. The rate and magnitude of expansion at an early age (the first two days of hydration) are higher when silica fume is added to the expanding cement paste. Solid phase analysis and rate curves of the pastes also show that the addition of silica fume accelerates the hydration of the paste [21]. Studies related to pore fluid analysis show that in expanding type K cement paste without silica fume, ettringite formation and subsequent expansion cease due to depletion of SO_4^{2-} in the pore fluid after 11 days of hydration. In the presence of silica fume, the initial formation of ettringite is accelerated, which leads to an increase in the rate and magnitude of expansion [22]. However, as shown in [23], in the case of using high-calcium fly ash as an independent binder, silica fume is an agent that blocks the expansion of fly ash mixtures. The low hardening rate and low strength of the fly ash-silica binder suggests the study of additives that accelerate the hardening of cement compositions.

One of the accelerating agents is calcium nitrate, which effectively increases the setting and hardening rate of Portland cement. The mechanism of action of $Ca(NO_3)_2$ in the cement paste is to increase the concentration of Ca^{2+} ions, which contributes to the saturation of the solution and more rapid formation of $Ca(OH)_2$ [24]. A comparison of three accelerating agents for pozzolanic Portland cement [25] shows that calcium nitrate is inferior in efficiency to calcium formate, which, in turn, is inferior to triethanolamine in the compressive strength of the cement mortar. It should be borne in mind that the effectiveness of calcium nitrate depends on the type of cement used. The results [26] show that calcium nitrate itself acts as a set accelerator, but it has a relatively small positive effect on the long-term development of mechanical strength. The combined addition of calcium nitrate and triisopropanolamine has shown significant and promising results at a very early age in terms of both setting acceleration and hardening acceleration.

The effect of calcium nitrate on white Portland cements is presented in [27] in various compositions of fresh cement paste after 7 and 28 days of hardening. The addition of calcium nitrate reduced the settling time and setting time of the specimens. In addition, the smaller size of the ettringite needles was established, and the plasticizing effect of calcium nitrate observed at an early stage of hydration. Flexural and compressive tests on cement specimens without the addition of sand or aggregates were carried out after curing at 7 and 28 days. The results showed a non-monotonic evolution of mechanical strength with calcium nitrate content. Diffractometry, SEM, and NMR relaxometry performed on specimens after final bending tests revealed changes in C-S-H gel morphology, an increase in the proportion of capillary pores, and an increase in the degree of carbonation with calcium nitrate content for older specimens.

Tests of commercial CEM I 52.5 R show that $Ca(NO_3)_2$ accelerates the silicate reaction and significantly influences the initial formation of the AFm and ettringite phases. In the presence of $Ca(NO_3)_2$, the dissolution rates of gypsum and anhydrite increase, and the formation of ettringite increases, especially at the highest analyzed dosage of 5 % $Ca(NO_3)_2$ by weight. In addition, significant amounts of NO_3-AFm are formed in the presence of $Ca(NO_3)_2$. Calcium nitrate shortens the time it takes for alite to rapidly hydrate. In addition to a significant increase in Ca^{2+} ions, there is a decrease in the concentration of Al^{3+} in the pore solution, which can also accelerate the hydration of alite in the presence of $Ca(NO_3)_2$ [28]. An increase in

the amount of ettringite present in the cement structure in the form of non-oriented needles is evidenced by SEM micrographs taken on the 28th day of cement slurry curing using NC [29].

A study [30] considers class C fly ash in the presence of various concentrations of calcium nitrate. Tests have shown that calcium nitrate accelerates the hydration of the calcium aluminate phases with respect to dosage. The new products consist of calcium aluminate hydrate and nitrate. Evidence suggests that modified nitrate hydrates compete with or inhibit calcium aluminate sulfate hydrates.

The work aims to study the effect of $Ca(NO_3)_2$ additive on the strength, heat of hydration, and phase composition of hydration products of the binder based on high-calcium fly ash and silica fume.

Tasks of the research:

1. Determination based on the results of X-ray Diffraction Analysis (XRD) what interactions occur in the "fly ash – silica fume – $Ca(NO_3)_2$" system and how these interactions affect the hydration.
2. Differential Thermal Analysis (DTA) of cementless binder specimens with different content of $Ca(NO_3)_2$ additive.
3. Experimental study of the $Ca(NO_3)_2$ additive on the heat release of cementless binder.
4. Experimental study of the effect of the $Ca(NO_3)_2$ additive on the compressive strength of specimens from a mortar with polyfractional standard sand.

2. Materials and Methods

2.1. Characteristics of Fly Ash Collected from Electrostatic Precipitators

The work uses high-calcium fly ash from Berezovskaya Thermal Power Plant. The bulk density is 1.09 g/cm^3, the true density is 3.09 g/cm^3, the median particle size is 7.7 μm, and the Blaine specific surface area is 2815 cm^2/g. The chemical composition of coal fly ash from the Berezovsky deposit is given in Table 1.

Table 1. Chemical composition of the fly ash specimen.

CaO	SiO_2	Al_2O_3	Fe_2O_3	MgO	P_2O_5	SO_3	K_2O	Na_2O	Chlorine ion	C	Loss on ignition
42.2	26.8	6.49	6.09	7.05	<0.1	2.86	0.23	0.43	<0.05	2.33	3.44

The results of X-ray diffraction analysis (XRD) obtained earlier in [23] showed that about 15 % of free calcium oxide is contained in fly ash. In addition, the main minerals of this fly ash include aluminates, silicates, aluminosilicates, calcium ferrites, and aluminum and magnesium oxides (Table 2). TiO_2, MnO_2, P_2O_5 are present in small amounts. Minerals such as brownmillerite, andradite, merwinite, grossular, and quartz have been identified [23].

High-calcium fly ash, when mixed with water, seizes and hardens. However, due to the presence of a large amount of free lime, its hardening is accompanied by strong expansion and cracking.

Table 2. Composition of fly ash according to X-ray phase analysis.

Crystal phases	Chemical composition of phases	Conditional content [%]
Lime	Ca O	62.39
Graphite	C	12.81
Periclase	Mg O	7.3
Brownmillerite	$4CaO{\cdot}Al_2O_3{\cdot}\ Fe_2O_3$	3.71
Andradite	$3CaO{\cdot}Fe_2O_3{\cdot}3SiO_2$	3.62
Merwinite	$3CaO{\cdot}MgO{\cdot}2SiO_2$	3.39
Millosevichite	$Al_2(SO_4)_3$	1.97
Calcium Aluminum Oxide	$3CaO{\cdot}Al_2O_3$	1.92
Grossular	$3CaO{\cdot}Al_2O_3{\cdot}3SiO_2$	1.06
Aluminum Oxide	Al_2O_3	0.54
Yeelimite	$3CaO{\cdot}Al_2O_3{\cdot}CaSO_4$	0.51
Kilchoanite	$3CaO{\cdot}2SiO_2$	0.41
Quartz	SiO_2	0.38

The X-ray diffraction pattern corresponding to Table 2 is shown in Fig. 1.

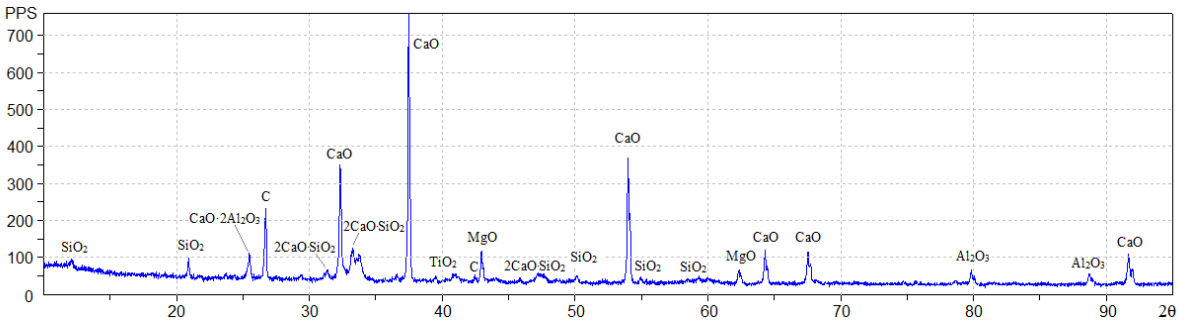

Figure 1. X-ray diffraction pattern of fly ash.

2.2. Determination of Compressive Strength

The compressive strength of the specimens consisting of fly ash-silica fume binder with $Ca(NO_3)_2$ additive was determined on test cube with dimensions of 32×32×32 mm. 4 mixtures were tested, differing in the dosage of $Ca(NO_3)_2$ additive (from 1.5 to 11.8 % of the fly ash mass). The content of silica fume in the mixture was 30.4 % of the fly ash mass. The additive was introduced into the mixture in the form of an aqueous solution. The water content in the solution was considered in the calculation of the water/binder ratio (W/B). The water content in the finished mixture was selected so as to obtain mixtures with the same consistency. At the same time, W/B increases with increasing dosage of $Ca(NO_3)_2$ from 0.41 to 0.43. 6 specimens of each mixture were prepared. Demolding of the specimens was carried out after 2 days. Immediately after demolding, 3 out of 6 specimens were placed in water, and the other 3 were left to harden in sealed containers. This prevented the specimens from drying out and excluded their contact with the outside air in the laboratory, the temperature of which was regulated and amounted to (20±2) C. The specimens of both dry and wet hardening were tested for compressive strength after 7 days from the date of manufacture. Before testing, the state of the specimens was visually assessed, the presence of expansion and cracks.

The compressive strength of the specimens of fly ash-sand mortar (Table 3) was determined on test cube with dimensions of 7×7×7 cm. Specimens were tested at the age of 28 days, in the amount of 3 pieces per test. The specimens were stored in a laboratory room with a temperature of (20 ± 2) °C, for the first 7 days in covered forms, and the rest of the time in a desiccator above water.

Table 3. Compositions and designation of specimens for determining strength and heat release.

Material	Consumption of materials [kg/m^3]		
	Q1	Q4	Q6
Fly ash	210	210	210
Silica Fume MKU-85	-	90 (42.9 %)	90 (42.9 %)
$Ca(NO_3)_2$ (dry)	-	-	24.8 (11.8 %)
Polyfractional sand	1645	1476	1451
Water	318	340	330
Total	2173	2116	2106

The compressive strength of all specimens was determined using a PGM-50MG4 hydraulic test press with a maximum force of 50 kN. During the test, the loading rate was maintained (50±10) kPa/s.

2.3. Influence of Calcium Nitrate on Phase Composition of Hydration Products of Fly Ash-Silica Fume Binder

The use of X-ray diffraction analysis and differential thermal analysis was aimed at establishing what interactions occur in the fly ash–silica fume– $Ca(NO_3)_2$ system and how they affect the hydration and strength of the fly ash stone. Both analyzes were performed as described in [23].

The analyses were performed on specimens of the fly ash-silica fume binder compositions listed in Table 4.

Table 4. Component content of binder.

Component type	Component content in composition of binder [%]		
	Mix 1	Mix 2	Mix 3
Fly ash	100	70	64.7
Silica Fume MKU-85	–	30	27.7
$Ca(NO_3)_2$	–	–	7.6
Water-solid ratio	1.2	0.42	0.50

Semiquantitative analysis of crystalline phases in the specimens was carried out on a Dron 7 X-ray diffractometer produced by JSCE "Burevestnik"(Russia) with the following parameters: CuKα radiation, λ = 0.15406 Å, 2θ shooting range from 8° to 94° with a step of 0.02°, and an exposure of 3 and 5 s.

Differential thermal analysis (DTA) was performed on the device "Termoscan" produced by LLC "Analitpribo" (Russia). The specimens for DTA had a mass of about 0.7–0.8 g. The specimens were heated to a temperature of 950–1000 °C.

2.4. Influence of Calcium Nitrate on Heat release of Fly Ash-Silica Fume Binder

The heat release of the specimens consisting of fly ash-silica fume binder and sand was determined experimentally by the semi-adiabatic (thermos) method according to EN 196-9:2010. The test procedure is described in detail [23]. To obtain comparable results, the heat release of concrete obtained by the semi-adiabatic method at an initial concrete temperature of 20 C was calculated to an isothermal hardening regime at a temperature of 20 C using the reduced time hypothesis [31].

The heat release of the binder was determined in the composition of a mortar with standard polyfractional sand on cylindrical specimens with a diameter of 62 mm and a height of 160 mm. Three compositions of the mortar were tested (designation Q1, Q4, Q6) with the same amount of fly ash, but with a different combination of additives (Table 3).

3. Results and Discussion

3.1. Compressive strength test results

The test results are shown in Table 5. For comparison Table 5 also shows the strength of the same fly ash-silica binder with the addition of $MgCl_2$ according to [23].

Table 5. Compressive strength of specimens with different accelerating agents.

$Ca(NO_3)_2$ content [% by weight of fly ash]	Compressive strength [MPa]			
	$Ca(NO_3)_2$		$MgCl_2$	
	dry	in water	dry	in water
1.5	3.5	0	2.9	0
4.7	2.7	0	8.3	0
8.2	8.8	0.38	9.8	1.92
11.8	10.4	1.15	15.2	2.3

The addition of $Ca(NO_3)_2$ showed a relatively low result compared to the addition of $MgCl_2$. With the same additive content of 11.8 %, the compressive strength of the specimens was 10.4 and 15.2 MPa, respectively.

The appearance of specimens with $Ca(NO_3)_2$ is shown in Fig. 2. It can be seen that the specimens of dry hardening with a low content of $Ca(NO_3)_2$ (1.5 % and 4.7 %) underwent cracking. In water, specimens of these compounds swelled and cracked even more. Specimens with a high content of $Ca(NO_3)_2$ (8.2 %–11.8 %) passed the test without cracking during dry hardening. In water, however, there was a slight expansion of these specimens and slight cracking.

The addition of $Ca(NO_3)_2$ is inferior in strength to magnesium chloride, but unlike chloride salts, it does not cause corrosion of steel reinforcement and therefore can be considered as an accelerator for reinforced concrete. Calcium nitrate does not cause cracking and expansion at high dosages (8.2%–11.8 %) and dry curing conditions, however, does not provide water resistance (Fig. 2). The softening coefficient is 0.04–0.11.

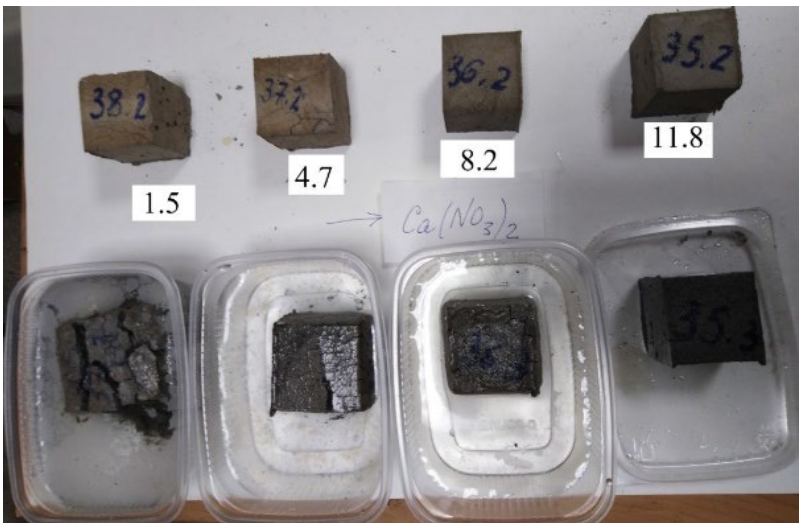

Figure 2. Specimens with $Ca(NO_3)_2$ additive. The top row is specimens hardening in dry conditions; bottom row is specimens hardening in water.

3.2. Results of X-ray diffraction analysis

X-ray patterns of the specimens of mixes presented in Table 4 after curing are shown in Fig. 3.

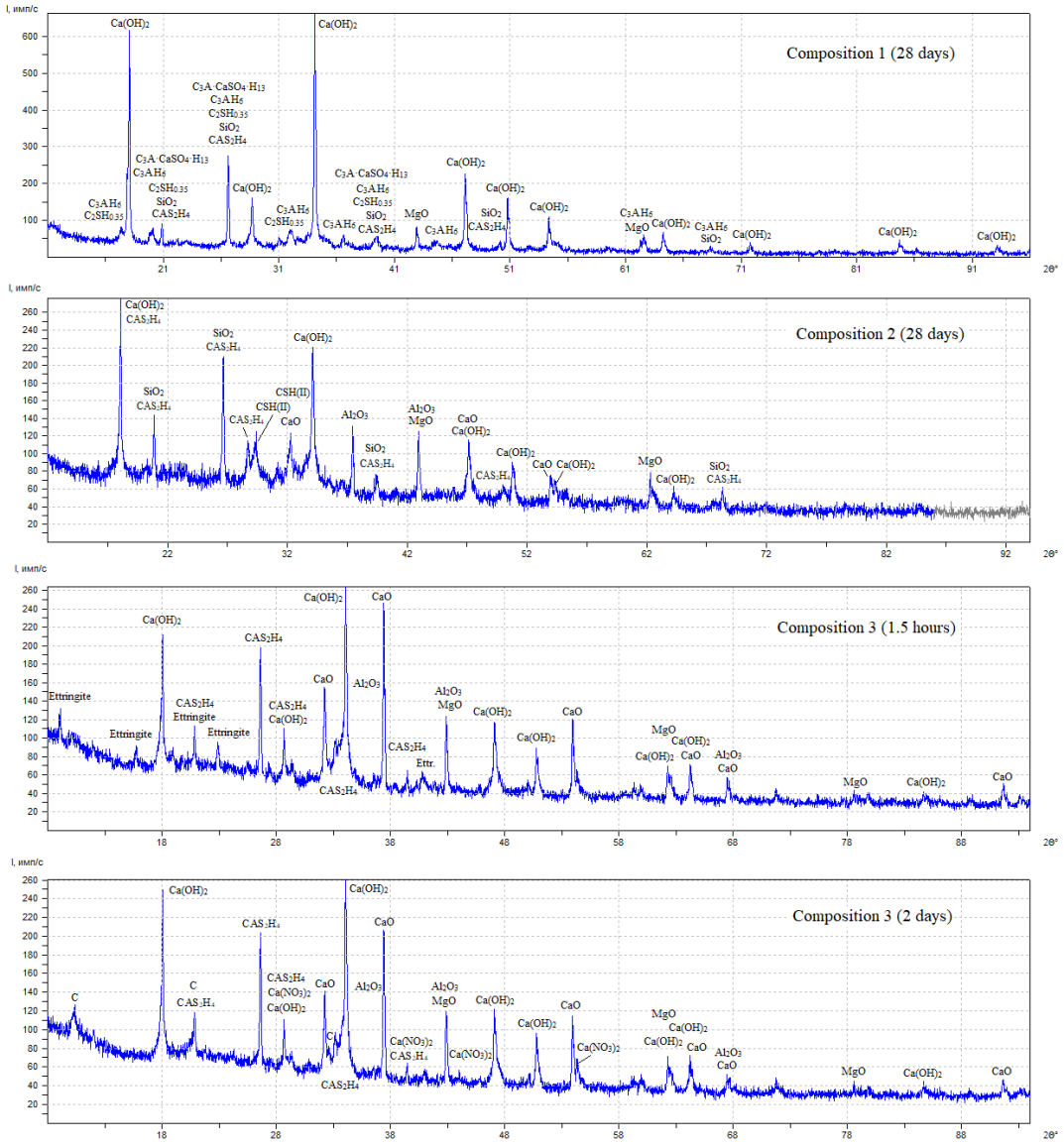

Figure 3. X-ray diffraction pattern of mixes after curing (Table 4).

A semi-quantitative analysis was carried out using the integral values of the intensity of the X-ray peaks. The obtained conditional values of the percentage of identified hydrated phases are given in Table 6.

Table 6. Conventional values of percentage of identified phases.

Phase	Chemical composition of phase	Mix 1 (28 days)	Mix 2 (28 days)	Mix 3	
				1.5 h	2 days
Lime	CaO	-	12.8	43.0	30.2
Portlandite	$Ca(OH)_2$	85.4	41.8	37.2	35.0
Katoite	C_3AH_6	11.1	-	-	-
Gismondine	CAS_2H_4	-	27.5	11.2	18.9
Calcium Aluminum Silicate Hydrates	CAS_6H_4	-	-	-	7.1
Katoite silication	C_3ASH_4	-	2.7	-	-
Calcium Silicate Hydrates	CSH(II)	-	15.2	-	8.7
Calcium Aluminum Oxide Sulfate Hydrate	$C_3A{\cdot}CaSO_4{\cdot}H_{13}$	3.5	-	-	-
Ettringite	$C_3A{\cdot}3CaSO_4{\cdot}H_{32}$	-	-	8.6	-

Consideration of the data in Table 6 allows us to draw the following conclusions.

1. In the absence of silica fume and $Ca(NO_3)_2$ (mix 1), the interaction of fly ash with water for 28 days led to the complete hydration of CaO_{free}. At the same time, calcium hydroxide was formed in the overwhelming amount from the products of hydration. Its amount was 85.4 % of the mass of the identified phases. Hydrosilicates in crystalline form were not found. Of the calcium hydroaluminates, C_3AH_6 was present (11.1 %). A small proportion (3.5 %) was the low sulfate form of calcium hydrosulfoaluminate.

2. The addition of silica fume to the fly ash (mix 2) slowed down the hydration of lime. This corresponded to the effect of silica impurities on the rate of quenching of air lime. After 28 days of hydration, the fly ash still contained a significant amount of unreacted CaO_{free} (12.8 %) and the $Ca(OH)_2$ content almost halved compared to mix 1 as a result of the action of silica fume. This was indicated by the significant content of calcium silicates and aluminosilicates formed. The effect of silica fume on the hydration of high-calcium fly ash was considered by us in more detail in [23].

3. The effect of $Ca(NO_3)_2$ (mix 3) was investigated for two hydration periods. After 1.5 hours, a significant amount of unreacted CO_{free} (43 %) remained in the binder, and 37.2 % $Ca(OH)_2$ was formed. Calcium silicate hydrates were absent, which was explained by insufficient time for reactions to occur and crystallization of hydration products. An analysis of the literature shows that, the interaction between $Ca(OH)_2$ and SiO_2 was noticeable approximately 3 days after the onset of hydration. Aluminosilicate CAS_2H_4, corresponding in composition to the natural mineral Gismondine, and calcium hydrosulfoaluminate of the trisulfate form (ettringite) were quite clearly identified. By the age of 2 days, calcium silicate hydrates of the tobermorite group CSH(II) according to Taylor were formed, the content of gismondine increased, and calcium aluminosilicate of composition CAS_6H_4 appeared.

A semi-quantitative X-ray phase analysis was also carried out for specimens of fly ash-silica fume binder with the calcium nitrate additive, which were previously tested for strength (Table 5). The results of X-ray phase analysis are given in Table 7, and the X-ray diffraction pattern is given in Fig. 4.

Table 7. Conventional values of percentage of identified phases resulting from hydration of binder consisting of fly ash and silica fume.

Phase	Chemical composition of phase	Dry curing				Water curing	
		$Ca(NO_3)_2$ content [% by weight of fly ash]					
		1.5	4.7	8.2	11.8	1.5	11.8
Portlandite	$Ca(OH)_2$	47.4	34.0	24.4	20.8	33.6	32.1
Lime	CaO	21.8	21.1	25.6	17.4	6.8	3.5
Calcite	$CaCO_3$	0.8	0.7	9.7	2.0	13.2	0.8
Ettringite	$C_3A{\cdot}3CaSO_4{\cdot}H_{32}$	8.4	9.4	14.2	9.3	10.8	10.8
Gismondine	CAS_2H_4	-	8.7	23.9	37.2	8.2	21.5
Yugawaralite	CAS_6H_4	7.9	-	2.2	1.0	2.9	3.9
Goosecreekite	CAS_6H_5	-	16.6	-	12.4	9.5	7.7
Calcium Silicate Hydrate	CSH(II)	13.8	9.6	-	-	15.0	19.7

Table 7 shows only those phases that are formed in the binder as a result of hydration and accompanying reactions and which are most often repeated in the studied compositions. The total content of these phases is taken as 100 %.

The main identified phases that satisfy this condition are lime, calcium hydroxide, ettringite, CSH(II) type silicates, and calcium aluminosilicates corresponding to such minerals as gismondine, yugavaralite, and goosecreekite. The influence of $Ca(NO_3)_2$ on CaO hydration during dry hardening is manifested to a small extent. The residual content of free lime slightly fluctuates relative to the average value of 21.4 % with a tendency to decrease with an increase in the $Ca(NO_3)_2$ amount. With water curing, the amount of lime is sharply reduced to an average of 5.2 %. In this case, an increase in the dosage of $Ca(NO_3)_2$ from 1.5 to 11.8 % leads to a decrease in the CaO content by almost 2 times. With an increase in the dosage of calcium nitrate, the content of portlandite noticeably decreases, obviously due to the reaction with silica, and the amount of calcium hydroaluminosilicates increases significantly, the total content of which increased by 6.4 times during dry curing, and 1.6 times during water curing. However, calcium hydrosilicates during dry storage are observed only in the case of a low dosage of $Ca(NO_3)_2$ additive (1.5 % and 4.7 %). At higher dosages they are not identified. Specimens hardened in water show the presence of hydrosilicates in a significant amount and, the greater, the higher of the additive content. Ettringite does not show a pronounced dependence on the additive dosage and hardening conditions; its content in all compositions remained approximately the same. Thus, the addition of calcium nitrate mainly intensifies the formation of calcium aluminosilicate hydrates, especially of the composition CAS_2H_4. Reaction products of $Ca(NO_3)_2$ with calcium silicates and aluminates, such as calcium hydroxynitrates and hydronitroaluminates, which are usually formed during hardening of Portland cement with the calcium nitrate addition, are not found. Perhaps their formation occurs at the molecular level in the form of X-ray amorphous mass.

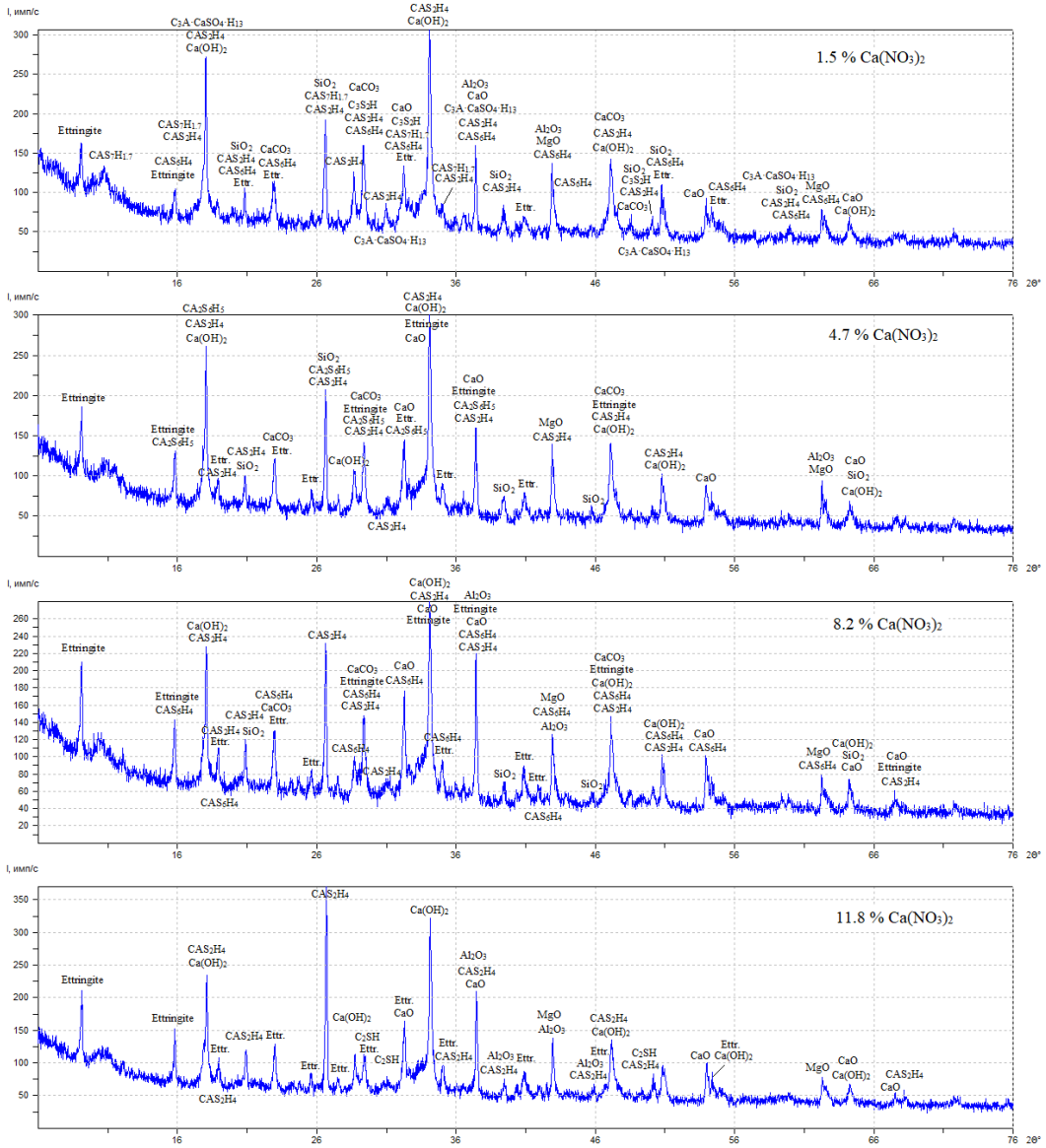

Figure 4. X-ray diffraction pattern of mixes with $Ca(NO_3)_2$ additive pre-tested for strength (Table 5).

3.3. Results of differential thermal analysis

Fig. 5 shows the DTA curves for mixes 2 and 3 at different ages (Table 4).

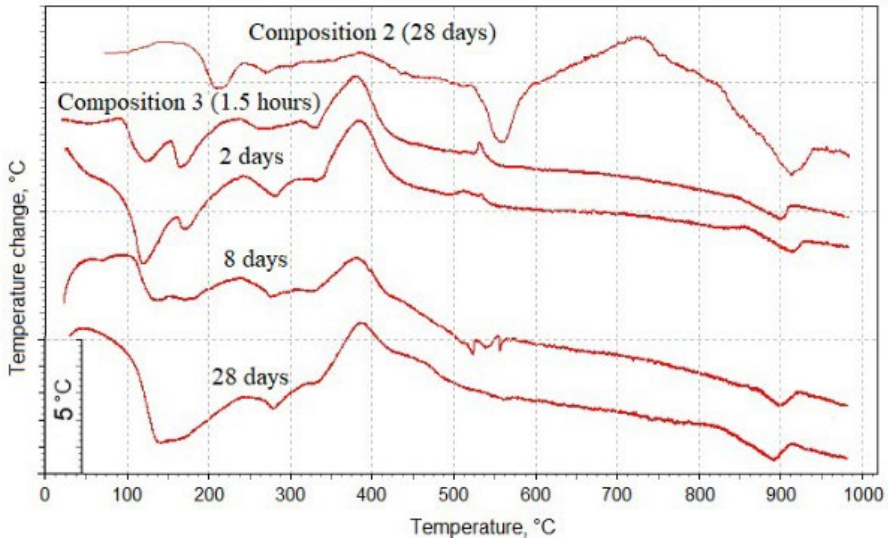

Figure 5. DTA curves of mix 2 (without $Ca(NO_3)_2$) and mix 3 with $Ca(NO_3)_2$ additive of 11.8 % at different ages.

The thermogram of mix 2 shows 3 pronounced endothermic peaks at 210, 560, and 915 °C. The first of them may correspond to the loss of interlayer water in tobermorite. The effects at 560 and 915 °C refer to the decomposition of $Ca(OH)_2$ and $CaCO_3$, respectively. The exoeffect at 730 °C shows the presence of tobermorite in mix 2, which transforms into wollastonite — $5CaO{\cdot}6SiO_2{\cdot}9H2O$.

Other thermograms show a number of effects caused by the $Ca(NO_3)_2$ influence. There are two endothermic peaks in the temperature range of 120–180 °C, which may be associated with the presence of gypsum and the reaction of ettringite formation. It is possible that gypsum is formed as a result of the reaction of $Ca(OH)_2$ with aluminum sulfate. The intensity of the first endoeffect increases with the specimens age, which may indicate an increase in the ettringite amount. The decrease in the second peak intensity is associated with the consumption of gypsum for the reaction. In this temperature range, the loss of adsorbed and interlayer water by hydrosilicates also usually occurs. The effect at 170–180 °C may be associated with the dehydration of the CAS_2H_4 compound or other calcium alumina hydrosilicates. Endothermic peak at 280 °C observed after cement hydration for 5 hours, O.P. Mchedlov-Petrosyan et al. attribute the presence of C_2AH_7 [32]. The authors of [33] believe that at a temperature of about 280 °C, the process of dehydration of C_2AH_8 and CAH_{10} begins. Endothermic peaks at 140, 280, and 560 °C can also be attributed to calcium hydronitroaluminate $C_3A{\cdot}Ca(NO_3)_2{\cdot}10H_2O$.

A slight endothermic effect at 330–340 °C is associated with C_3AH_6 presence, and an exothermic peak at 380 °C indicates the transformation of soluble anhydrite into insoluble one.

The thermograms of mix 3 (Fig. 5) show almost no endothermic effect of $Ca(OH)_2$ decomposition, although according to X-ray diffraction analysis, it should be present. At the same time, in the temperature range of 520–550 °C, small areas of exothermic peaks are observed, which are superimposed on the effect of $Ca(OH)_2$ dehydration, blocking the heat input for the decomposition of portlandite. Since mix 2 does not show a similar effect, the addition of calcium nitrate can be considered responsible. Unfortunately, it has not yet been possible to decipher this exoeffect. Probably in this case, the burnout of unburned carbon particles occurs.

The thermograms shown in Fig. 6 characterize the effect of the $Ca(NO_3)_2$ dosage on the phase composition of the specimens consisting of fly ash, silica fume and $Ca(NO_3)_2$ additive.

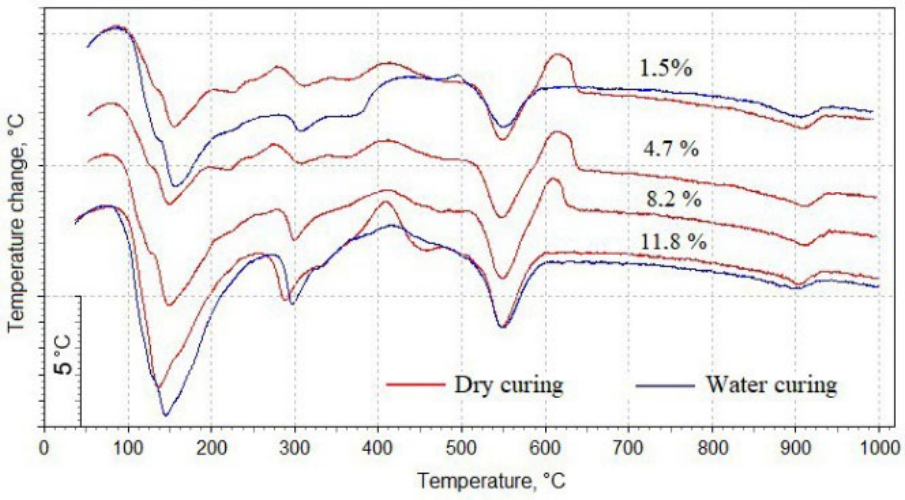

Figure 6. DTA curves of specimens with different content of calcium nitrate.

Fig. 7 shows that with an increase in the $Ca(NO_3)_2$ content, the depth of the endothermic peak sharply increases at a temperature of about 150 °C, which indicates an increase in the growth of hydrates of aluminates and calcium aluminosilicates in the presence of $Ca(NO_3)_2$. In this case, the intensity of the endothermic peak at 550 °C corresponding to the decomposition of $Ca(OH)_2$ decreases. In these specimens, after 7 days of hydration, two endothermic effects at temperatures around 300 and 460 °C can be attributed to cubic C_3AH_6. The peak at 300 °C can also be seen as offset from the effect at 280 °C in the previous diagram (Fig. 5). On the thermograms in Fig. 7, two exothermic peaks are observed. The first one, at 410 °C, is especially pronounced on the curve for the mix with the highest content of the $Ca(NO_3)_2$ additive (11.8 %) during dry hardening. On thermograms with a lower content of calcium nitrate, this effect is more blurred and insignificant. A similar exothermic effect (also at 11.8 % $Ca(NO_3)_2$) is observed on thermograms for mix 3 at the age from 1.5 h to 28 days, however, at 280 °C (Fig. 5). The second exothermic peak on the thermograms of the dry curing specimens with the addition of 1.5–8.2 % $Ca(NO_3)_2$ at 610–620 °C is presumably associated with the burnout of carbonaceous particles.

3.4. Results of Heat Release Determination

The specific heat release of a mortar consisting of fly ash and sand, per 1 kg of fly ash at a temperature of 20 °C, depending on the composition, is shown in Fig. 7.

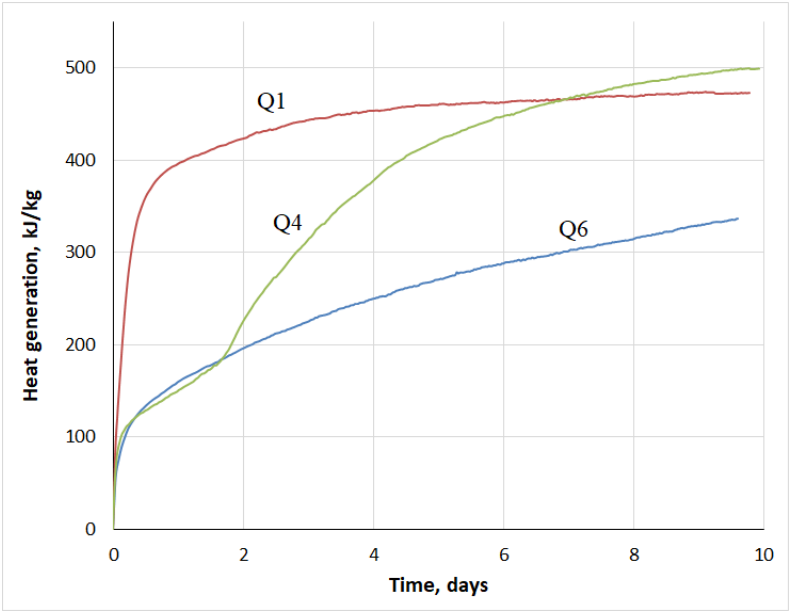

Figure 7. Specific heat release of mortar per 1 kg of fly ash at temperature of 20 °C, depending on composition: Q1 is mix without additives; Q4 is mix with MS additive of 42.9 %; Q5 is mix with additives: MS of 42.9 % and $Ca(NO_3)_2$ of 11.8 %.

Pure fly ash (curve Q1) reacts very violently with water due to the slaking of free lime. Approximately 1 day after intense heat release, the process slows down sharply and ends by the fourth day. In the

presence of silica fume (curve Q4), a sharp slowdown of the heat release process is observed. By the end of the second day, the reaction rate increases again and on the 10th day the heat release is higher than that of pure fly ash. The addition of $Ca(NO_3)_2$ (curve Q6) provides a reduced heat release of the mortar. In the initial period up to 1.5 days, curves Q4 and Q6 practically coincide. This indicates that the hydration process during this period is controlled by silica fume, and the retarding effect of calcium nitrate begins to affect later. At the same time, the heat release rate (the angle of inclination of the tangent to curves Q4 and Q6) for mix Q6 is higher than for mix Q4, and it should be expected that by a certain long term of hydration, the integral values of their thermal effects will become equal. Thus, the $Ca(NO_3)_2$ additive blocks the accelerating effect of silica, starting from 1.5-2 days of hydration.

Heat release experiments require a certain amount of time for preparing the mix, preparing the specimens, placing the specimens in thermoses, etc. In our case, this time is about 30 minutes. During this period, intense heat release occurs, however, it is not recorded in the experiment. Therefore, we made additional tests to increase the temperature of the paste based on fly ash and additives during the first 1 hour of hydration. The mixes of the test are given in Table 8.

Table 8. Mixes for determining temperature in initial period of hydration.

Material	Consumption of materials [kg/m^3]		
	T1	T4	T6
Fly-ash	30	30	30
Silica Fume MKU-85	–	12.9 (42.9 %)	12.9 (42.9 %)
$Ca(NO_3)_2$ (dry)	–	–	3.54 (11.8 %)
Water	19.5	27.9	30.2
Total	49.5	70.8	76.64

The test procedure was presented in detail in [23]. Each mix was tested twice and the average value was taken. The results of measuring the temperature of the paste consisting of fly ash and silica fume are shown in Fig. 8.

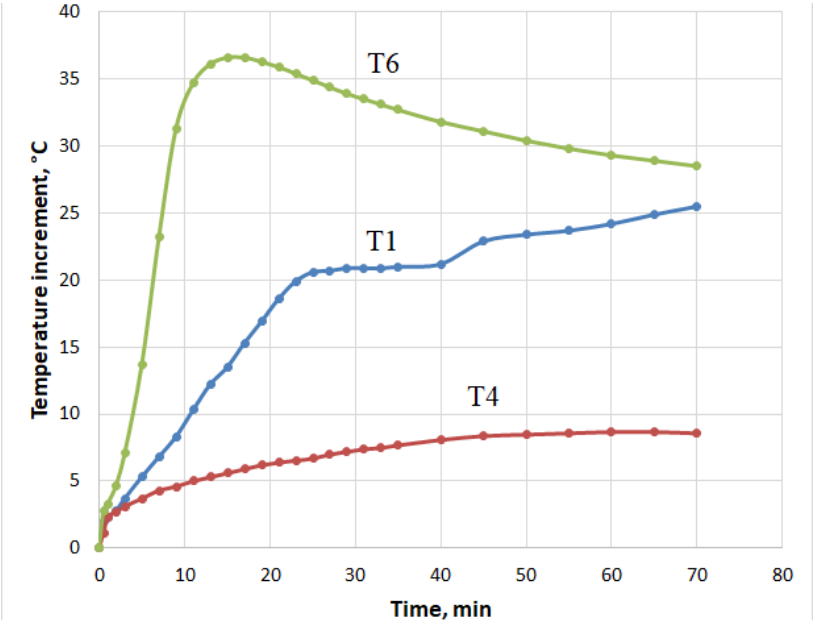

Figure 8. Temperature increase of specimens depending on mix: T1 is fly ash without additives; T4 is fly ash with MS additive of 42.9 %; T6 is fly ash with MS additive of 42.9 % and $Ca(NO_3)_2$ additive of 11.8 %.

Fig. 8 shows that the temperature of the fly ash (mix T1) for 1 hour of hydration increased by 24.2 °C against the initial one. At the same time, in the presence of silica fume (mix T2), the hydration rate dropped sharply, and the temperature of the paste increased by only 8.7 °C. Here, the same regularity of silica fume effect was observed as in the initial period of hardening of the mortar consisting of fly ash and silica fume (Fig. 7). The introduction of the $Ca(NO_3)_2$ additive led to an exceptionally sharp rise in temperature in the first 15 min after mixing. The temperature increase during this time was 36.6 °C.

Thus, calcium nitrate is a strong accelerator of the initial stage of the hydration process, which can be estimated at 30–60 minutes. After the initial stage, up to a period of about 1.5 days, there follows a

period when the heat release of binder, both with and without the $Ca(NO_3)_2$ additive, proceeds practically at the same level. That is, the supplement during this period does not accelerate or slow down the hydration process. In the next third period, a low monotonous increase in heat release Q6 continues (Fig. 7), while the composition without additive shows a sharp increase in heat release (curve Q4)

3.5. Influence of Calcium Nitrate on Strength of mortar consisting of Fly Ash and Sand

The results of determining the compressive strength of the specimens are shown in the diagram in Fig. 9.

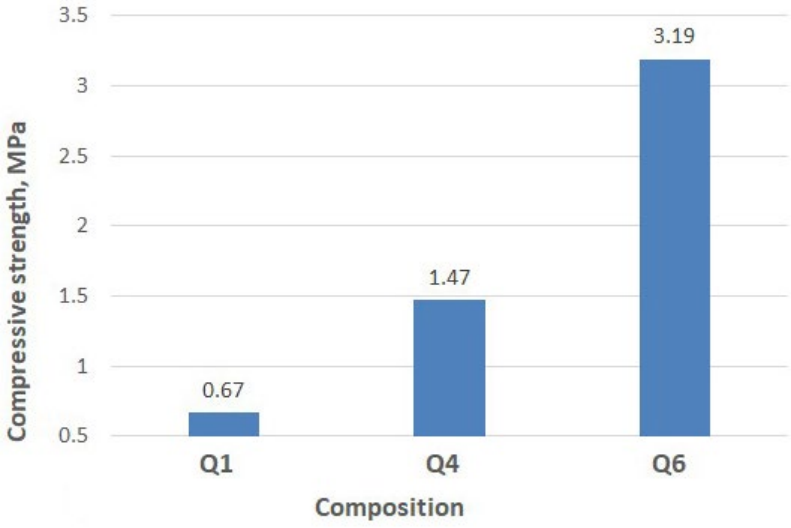

Figure 9. The results of determining compressive strength of specimens of mortar: Q1 is mix without additives; Q4 is mix with MS additive of 42.9 %; Q5 is mix with additives: MS of 42.9 % and $Ca(NO_3)_2$ of 11.8 %.

Fig. 9 shows, that the silica fume additive increased the strength of the specimens by approximately 100 %, and when $Ca(NO_3)_2$ was added to the mortar consisting of fly ash, silica fume and sand, the strength increased by more than two times.

It should be noted the low strength of the tested mixes of the mortar, however, it must be borne in mind that the binder/sand ratio in these mixes ranges from 1:5 to 1:7.

4. Conclusions

This paper presented the results of experimental studies conducted to evaluate the influence of $Ca(NO_3)_2$ additive on the strength, heat of hydration, and phase composition of hydration products of the binder based on high-calcium fly ash and silica fume. The following key conclusions were drawn from this study:

1. The effect of $Ca(NO_3)_2$ (mix 3, Table 4) was studied using XRD and DTA. After 1.5 h of hydration, a significant amount of unreacted CO_{free} (43 %) remains in the paste and 37.2 % $Ca(OH)_2$ is formed. Aluminosilicate CAS_2H_4, corresponding in composition to the natural mineral gismondine, and calcium hydrosulfoaluminate of the trisulfate form (ettringite) are quite clearly identified. By the age of 2 days calcium silicate hydrates of the tobermorite group are formed, the content of gismondine increases, and calcium aluminosilicate of the composition CAS_6H_4 appears. The main phases identified in specimens aged 7 days at different $Ca(NO_3)_2$ content are lime, calcium hydroxide, ettringite, CSH(II) type silicates, and calcium aluminosilicates, corresponding to such minerals as gismondine, yugavaralite, and goosecreekite. The influence of $Ca(NO_3)_2$ on CaO hydration during dry hardening is manifested to a small extent. The residual content of free lime slightly fluctuates relative to the average value of 21.4 % with a tendency to decrease with an increase in the $Ca(NO_3)_2$ amount. With water curing, the amount of lime is sharply reduced to an average of 5.2 %. In this case, an increase in the $Ca(NO_3)_2$ content from 1.5 to 11.8 % leads to a decrease in the CaO content by almost 2 times. With an increase in the dosage of calcium nitrate, the content of portlandite noticeably decreases, obviously due to the reaction with silica, and a significant increase in the amount of calcium hydroaluminosilicates, the total content of which increased by 6.4 times during dry curing, and 1.6 times during water storage. The specimens hardened in water show the presence of hydrosilicates in a significant amount and in positive relation to the additive content. Thus, the calcium

nitrate additive mainly intensifies the formation of calcium aluminosilicate hydrates, especially of the composition CAS_2H_4.

2. With an increase in the $Ca(NO_3)_2$ content in the binder based on fly ash and silica fume after 7 days of hydration, the depth of the endothermic peak at 150 °C on the DTA curves increases, which confirms the intensive growth of hydrates of aluminates and calcium aluminosilicates in the presence of $Ca(NO_3)_2$. In this case, the intensity of the endothermic effect at 550 °C, corresponding to the decomposition of $Ca(OH)_2$, decreases. Two endothermic peaks are observed at temperatures around 300 and 460 °C, which may belong to cubic C_3AH_6. There are also two exothermic peaks. The first one, at 410 °C, increases with the content of the $Ca(NO_3)_2$ additive. Its nature has not been elucidated. The second exothermic peak at 610–620 °C is presumably associated with the burnout of carbonaceous particles.

3. A study of the heat release process showed that pure fly ash reacts very violently with water, due to the slaking of free lime. During the first day, 85 % of heat is released from the value for 10 days. Silica fume significantly slows down the heat release of fly ash in the initial period of hardening up to 1.5 days, after which a sharp rise follows, and by the end of the experiment, the heat release of the binder exceeds the value for pure fly ash. Calcium nitrate greatly accelerates the process in the first 60 minutes of hydration. However, then the mix with the $Ca(NO_3)_2$ additive is inferior in the rate of heat release to binder without additive.

4. When testing a mortar consisting of fly ash, silica fume and sand, the $Ca(NO_3)_2$ additive more than doubled the compressive strength of the mortar.

References

1. Ahmad, J., Zhou, Z., Usanova, K.I., Vatin, N.I., El-Shorbagy, M.A. A Step towards Concrete with Partial Substitution of Waste Glass (WG) in Concrete: A Review. Materials (Basel). 2022. 15(7). P. 2525. DOI: 10.3390/ma15072525
2. Ahmad, J., Martínez García, R., de Prado Gil, J., Irshad, K., El-Shorbagy, M., Fediuk, R., Vatin, N. Concrete with Partial Substitution of Waste Glass and Recycled Concrete Aggregate. Materials. 2022. 15. 430. DOI: 10.3390/ma15020430
3. Klyuev, S., Sevostyanov, V., Sevostyanov, M., Ageeva, M., Fomina, E., Klyuev, A., Protsenko, A., Goryagin, P., Babukov, V., Shamgulov, R., Fediuk, R., Sabitov, L. Improvement of Technical Means for Recycling of Technogenic Waste to Construction Fiber. Case Studies in Construction Materials. 2022. 16. e01071. DOI: 10.1016/j.cscm.2022.e01071
4. Petrov, V.V., Protsenko, A.E., Sapozhnik, K.R. Solid-cabide tool waste recycling technology. Construction Materials and Products. 2022. 5(3). Pp. 27–34. DOI|: 10.58224/2618-7183-2022-5-3-27-34
5. Zakrevskaya, L.V., Gavrilenko, A.A., Kapush, I.R., Lyubin, P.A. Creating ground concrete and strengthening substrates using mining waste. Construction Materials and Products. 2022. 5 (3). Pp. 35–44. DOI: 10.58224/2618-7183-2022-5-3-35-44
6. Kashapov, R.N., Kashapov, N.F., Kashapov, L.N., Klyuev, S.V., Chebakova, V.Yu. Study of the plasma-electrolyte process for producing titanium oxide nanoparticles. Construction Materials and Products. 2022. 5 (5). Pp. 70–79. DOI: 10.58224/2618-7183-2022-5-5-70-79
7. Kashapov, R.N., Kashapov, N.F., Kashapov, L.N., Klyuev, S.V. Plasma electrolyte production of titanium oxide powder. Construction Materials and Products. 2022. 5 (6). Pp. 75–84. DOI: 10.58224/2618-7183-2022-5-6-75-84
8. Barabanshchikov, Y., Usanova, K., Akimov, S., Uhanov, A., Kalachev, A. Influence of Electrostatic Precipitator Ash “Zolest-Bet” and Silica Fume on Sulfate Resistance of Portland Cement. Materials. 2020. 13(21). 4917. DOI: 10.3390/ma13214917
9. Fediuk, R., Smoliakov, A., Timokhin, R., Batarshin, V., Yevdokimova, Yu. Using thermal power plants waste for building materials. IOP Conference Series: Earth and Environmental Science. 2017. 87(9). 092010. DOI: 10.1088/1755-1315/87/9/092010
10. Salamanova, M., Murtazaev, S.-A., Saidumov, M., Alaskhanov, A., Murtazaeva, T., Fediuk, R. Recycling of Cement Industry Waste for Alkali-Activated Materials Production. Materials. 2022. 15(19). 6660. DOI: 10.3390/ma15196660
11. Klyuev, S.V., Kashapov, N.F., Radaykin, O.V., Sabitov, L.S., Klyuev, A.V., Shchekina, N.A. Reliability coefficient for fibreconcrete material. Construction Materials and Products. 2022. 5 (2). Pp. 51–58. DOI: 10.58224/2618-7183-2022-5-2-51-58
12. Alani, A., Lesovik, R., Lesovik, V., Fediuk, R., Klyuev, S., Amran, M., Ali, M., de Azevedo, A.R.G., Vatin. N.I. Demolition Waste Potential for Completely Cement-Free Binders. Materials. 2022. 15(17). 6018. DOI: 10.3390/ma15176018
13. Giergiczny, Z. Fly ash and slag. Cement and Concrete Research. 2019. 124. 105826. DOI: 10.1016/j.cemconres.2019.105826
14. Vatin, N., Barabanshchikov, Y., Usanova, K., Akimov, S., Kalachev, A., Uhanov, A. Cement-based materials with oil shale fly ash additives. IOP Conf Ser Earth Environ Sci. 2020. 578(1). 012043. DOI: 10.1088/1755-1315/578/1/012043
15. Shi, H.-S. Research on intrinsic characteristics and hydration properties of fly ash with high calcium oxide. Tongji Daxue Xuebao/Journal of Tongji University. 2003. 31(12). Pp. 1440–1443.
16. Shevchenko, V.A., Artemieva, N.A., Ivanova, L.A., Kiselev, V.P., Vasilovskaya G.V. Cement-free binder from ash-silica compositions. Modern problems of science and education. 2015. 1. Pp. 1–8.
17. Domanskaya, I., Oleynik, V., Minyazev, D. ICSC Problems and Perspectives of high-calcium fly ash from heat power plants in the composition of “green” building materials. E3S Web of Conferences. 2016. 6. 01014. DOI: 10.1051/e3sconf/20160601014
18. Chaunsali, P., Mondal, P. Physico-chemical interaction between mineral admixtures and OPC–calcium sulfoaluminate (CSA) cements and its influence on early-age expansion. Cement and Concrete Research. 2016. 80(1). Pp. 10–20. DOI: 10.1016/j.cemconres.2015.11.003
19. He, S., Zhu, X.Y., Bao, W.Z., Zhao, W.X., Jin, D.M. Study on Expansion of Circulating Fluidized Bed Combustion Coal Ash. Advanced Materials Research. 2012. 518–523. Pp. 3501–3506. DOI: 10.4028/www.scientific.net/AMR.518-523.3501
20. Bich Thi Nguyen, T., Chatchawan, R., Saengsoy, W., Tangtermsirikul, S., Sugiyama, T. Influences of different types of fly ash and confinement on performances of expansive mortars and concretes. Construction and Building Materials. 2019. 209. Pp. 176–186. DOI: 10.1016/j.conbuildmat.2019.03.032

21. Lobo, C., Cohen, M.D. Hydration of type K expansive cement paste and the effect of silica fume: I. Expansion and solid phase analysis. Cement and Concrete Research. 1992. 22(5). Pp. 961–969.
22. Lobo, C., Cohen, M.D. Hydration of type K expansive cement paste and the effect of silica fume: II. Pore solution analysis and proposed hydration mechanism. Cement and Concrete Research. 1993. 23(1). P. 104–114.
23. Barabanshchikov, Y., Usanova, K. Influence of Silica Fume on High-Calcium Fly Ash Expansion during Hydration. Materials. 2022. 15(10). 3544. DOI: 10.3390/ma15103544
24. Kicaite, A. The effect of calcium nitrate on the properties of Portland cement pastes and concrete hardening at low temperatures. Ceramics – Silikaty. 2020. 64(3). Pp. 1–9.DOI: 10.13168/cs.2020.0015
25. Derakhshani, A., Ghadi, A., Vahdat, S.E. Study of the effect of calcium nitrate, calcium formate, triethanolamine, and triisopropanolamine on compressive strength of Portland-pozzolana cement. Case Studies in Construction Materials. 2023. 18(18). e01799. DOI: 10.1016/j.cscm.2022.e01799
26. Chikh, N., Zouaoui, M., Aggoun, S., Duval, R. Effects of calcium nitrate and triisopropanolamine on the setting and strength evolution of Portland cement pastes. Materials and Structures. 2008. 41. Pp. 31–36. DOI: 10.1617/s11527-006-9215-8.
27. Rusu, M., Vulpoi, A., Vilau, C., Dudescu, M., Păşcuţă, P., Ardelean, I. Analyzing the Effects of Calcium Nitrate over White Portland Cement: A Multi-Scale Approach. Materials. 2022. 16(1). 371. DOI: 10.3390/ma16010371.
28. Dorn, T., Hirsch, T., Stephan, D. Working mechanism of calcium nitrate as an accelerator for Portland cement hydration. Journal of the American Ceramic Society. 2023. 106(1). Pp. 752–766.
29. Belmonte, I., Soler, M., Benito, F., Costa, C., López, C., Martin, J., Pacheco, V., Torrano, P. Mineralization Reaction of Calcium Nitrate and Sodium Silicate in Cement-Based Materials. Crystals. 2022. 12(4). 445. DOI: 10.3390/cryst12040445
30. Russell Hill, K.D. The interaction of calcium nitrate and a Class C fly ash during hydration. Cement and Concrete Research. 1996. 26(7). Pp. 1131–1143.
31. Zaporozhec, D.I. Osnovy teorii teplovydeleniya betona [Fundamentals of the theory of heat generation of concrete]. Doctor Thesis. Leningrad. 1965. 33 p. (rus)
32. Ramachandran, V.S. Applications of Differential Thermal Analysis in Cement Chemistry. Chemical Publishing Company, 1969. 328 p.
33. Krivopustov, D.Yu. Fazovye prevrashcheniya cementnogo kamnya na osnove alyuminatnogo klinkera [Phase transformations of cement stone based on aluminate clinker]. Mezhdunarodnaya nauchno-tekhnicheskaya konferenciya molodyh uchenyh BGTU im. V.G. Shuhova [Conference proceedings]. Belgorod. 2019. Pp. 2519–2522.

Information about authors

Kseniia Usanova,
ORCID: https://orcid.org/0000-0002-5694-1737
E-mail: plml@mail.ru

Yuriy Barabanshchikov, *Doctor of Technical Sciences*
ORCID: https://orcid.org/0000-0001-7011-8213
E-mail: ugb@mail.ru

Saurav Dixit,
E-mail: sdixit@ricssbe.edu.in

Received 20.07.2023. Approved after reviewing 15.09.2023. Accepted 21.09.2023.